Stochastic Differential Equation Modeling of Target Tracking Errors

1.0 ABSTRACT

SCIENTIFIC METHODS OF TEST AND EVALUATION FOR AIRCRAFT SYSTEMS ARE BASED ON MATHEMATICAL MODELS OF THE SYSTEM UNDER TEST (SUT) PERFORMANCE. STOCHASTIC DIFFERENTIAL EQUATIONS OFFER A PROMISING CANDIDATE TO MODEL SYSTEMS WHOSE OUTPUT IS AUTOCORRELATED AND CONVERGES TO A SPECIFIC VALUE OVER TIME. IN THIS PAPER, WE ASSUME SUT'S BEHAVIOR CAN BE MODELED AS A STOCHASTIC PROCESS. WE SHOW HOW ERROR PROCESSES (E.G ALONG- AND CROSS-TRACK ERRORS IN TARGET LOCATION ERRORS) CAN BE MODELED BY THE ORNSTEIN-UHLENBECK (OU) STOCHASTIC DIFFERENTIAL EQUATION (SDE) AND THE RESULTING ONE-DIMENSIONAL EUCLIDEAN ERROR CAN BE MODELED BY THE COX-INGERSOLL-ROSS (CIR) SDE. WE USE THIS RESULT TO QUANTIFY THE PERFORMANCE OF A SYSTEM FOR TEST AND EVALUATION PURPOSES. WE ALSO INTRODUCE A GENERIC METHOD OF CONTROL CHARTING FOR EVALUATING SDES. AN ILLUSTRATIVE EXAMPLE SHOWS THE APPLICATION OF THE PROPOSED METHODS FOR AIRCRAFT TRACKING PERFORMANCE EVALUATION.

Keywords: System Performance, Ornstein-Uhlenbeck, Cox-Ingersoll-Ross, statistical process monitoring, diffusion process, Kalman Filter errors, autocorrelated errors

2.0 INTRODUCTION

Many of today's aircraft systems use Kalman filters to obtain estimates of mission parameters of interest. For example, navigation solutions and the location of a target of interest. Kalman filters used in target tracking systems provide estimates that are autocorrelated with errors that become smaller as the aircraft nears the target location These characteristics make mean-reverting stochastic differential equations (SDEs, also known as diffusion processes) ideal candidates for analysis models. To date, diffusion processes have been applied mostly to either physical phenomena (e.g. gas dynamics), or economic variables (e.g. interest rate evolution). Literature is virtually non-existent in quantifying the performance of a mean-reverting process or its statistical process monitoring (SPM) in aircraft system test and evaluation. In what follows, we discuss the literature on process control and profile monitoring in evaluating and monitoring diffusion processes.

Control charts, also known as Shewhart charts (Shewhart, 1931), are statistical quality control tools used to determine whether a process is in a state of control and are typically depicted graphically. For many years, monitoring the performance of a process or product for a single quality characteristic at a given time/space was at the center of standard SPM application. However, it gradually became apparent that in practice, some process measurements followed functional relationships. These types of processes are known as 'profile,' 'signature,' or 'waveform' in the literature. Monitoring linear profiles has been thoroughly studied (Abbas et al., 2016; Jensen *et al*., 2006, 2008; Kang and Albin, 2000; Kim *et al*., 2003; Mahmoud and Woodall, 2004; Ren *et al*., 2018; Wang and Tsung, 2005). Williams *et al*. (2003) proposed a broad approach for handling nonlinear profile monitoring where separate nonlinear (NL) regression models are fitted to each profile. Williams *et al*. (2007) provided an application of NL profile monitoring to dose-response data. Two major assumptions of profile monitoring were that profiles and/or the measurement among profiles are independent of each other (Rassoul Noorossana et al., 2011). These assumptions are unrealistic for some real-life applications. Consequently, monitoring profiles with

autocorrelated data has received attention in recent years. Noorossana (2008) discussed the monitoring of autocorrelated linear profiles and Jensen and Birch (2009) proposed a linear mixed model to monitor the profiles when there was correlation within profiles. There are also some studies for complicated profiles that can be modeled by nonlinear functions (S. I. Chang and Yadama, 2010; ShingI. Chang et al., 2012; Jones and Rice, 1992; Moguerza et al., 2007; Vaghefi et al., 2009; Walker and Wright, 2002).

Although there are studies on non-linear profiles control charts with autocorrelation, these charting methods do not handle the Weiner process component present in diffusion models. Thus, their control charts, lacking a stochastic component, would likely result in higher false alarm rates. The only work directly related to control charting of diffusion processes we found was provided by Tsai *et al.* (2014). In Section 4 of this paper, we show the limitation of the charts provided by Tsai, which results in control limits that are either too wide or too narrow. In this paper, we introduce methods by which the performance of mean-reverting diffusion processes can be quantified and evaluated.

In Section 3 of this paper, we give a brief review of the mathematics behind the sum-square of standardized OU processes (S3OUP) and its relationship with the CIR process. In Section 4, we use results from Section 2 to develop methods for the quantification of CIR performance monitoring. In Section 5, we provide an example to demonstrate how the proposed methods can be used for testing and evaluation of a tracking system performance. Finally, in Section 6 we summarize results and potential future research topics in the area.

3.0 RELATIONSHIP BETWEEN ORNSTEIN -UHLENBECK AND COX-INGERSOLL-ROSS PROCESSES

In this section, we briefly review the properties of OU and Cox-Ingersoll-Ross (CIR) processes. Further details may be found in Chen and Scott (1992) and Longstaff and Schwartz (1992). The OU process developed by Leonard Ornstein and George Uhlenbeck, is a mean-reverting stationary Gauss–Markov process. It is mean- reverting in that realizations tend to drift towards its long-range mean function. The OU process is a modification of the Wiener process; different in that the process tends to drift to a central location, and this drift tendency is greater, the further any point is from the mean. The OU process is given by the stochastic differential equation $dX_t = -\beta(X_t - \alpha)dt + \sigma dW_t$, where $\beta > 0$ is the speed at which the process reverts to its long-run (asymptotic) mean $\alpha, \alpha \in \mathbb{R}$. The $\sigma^2, \sigma > 0$, is the instantaneous variation of the process. W_t is the Wiener process, where w_t is a time-continuous process, $w_0 = 0$,and $\Delta w_t = w_{t+u} - w_u$ are independent of past values w_s, $s \leq t$ and are normally distributed $N(0, u)$ and. Let $X_0 = x_0$ represent the initial or starting point of the process. Then, the solution of SDE is:

$$X_t = \alpha + (X_0 - \alpha)e^{-\alpha t} + \sigma \int_0^t e^{-\beta(t-s)}\, dW_s \qquad (1)$$

Equation (1) is a summation of the solution to an ordinary differential equation and the integral of a deterministic function with respect to a Wiener process with normally distributed increments. Therefore, the distribution of X_t, is normal. The conditional and asymptotic distributions of X_t are summarized in terms (2) and (3), respectively.

$$(X_t | X_0 = x_0) \sim N(\alpha + (x_0 - \alpha)e^{-\beta t}, \frac{\sigma^2}{2\beta}(1 - e^{-\beta t})) \qquad (2)$$

$$X_{t\to\infty} \sim N(\alpha, \frac{\sigma^2}{2\beta}) \qquad (3)$$

If we have *v* independent OU processes, we define the asymptotic distribution of each process by including index *i*, where *i=1, 2, ..., v*. The square of a standard normal distribution variate follows a Chi-square distribution with one degree of freedom. Thus $Z^2_{i,t\to\infty} = \left(X_{i,t} - \alpha_i\right)^2 / \frac{\sigma_i^2}{2\beta_i} \sim \chi^2_{i,(1)}$, *i=1,2 ,..., v*, where $Z^2_{i,t\to\infty}$ shows the asymptotic standard normal distribution associated with CIR process *i*, where α_i=1

and $\frac{\sigma_i^2}{2\beta_i} = 2$, the mean and variance of Chi-squared distribution with one degree of freedom. Since $Z^2_{i,t\to\infty}$, $i=1,\ldots,\nu$ are independent identically distributed (i.i.d) thus the distribution of $\sum_{i=1}^{\nu} Z^2_{i,t\to\infty}$ is $\chi^2_{(\nu)}$. Let's define $Y_{t\to\infty} = \sum_{i=1}^{\nu} Z^2_{i,t\to\infty}$, then $Y_{t\to\infty} \sim \chi^2_{(\nu)}$. Also, the chi-square distribution with ν degrees of freedom is a gamma distribution with shape parameters $\nu/2$ and 1/2. This relationship can then be summarized by $Y_{t\to\infty} \sim \chi^2_{(\nu)} = Gamma\,(\frac{\nu}{2}, \frac{1}{2})$. Since we know the underlying distribution of $Y_{t\to\infty}$, we can calculate $E[Y_t] = \nu$ and $var[Y_t] = 2\nu$. On one hand, the asymptomatic distribution of $Y_{t\to\infty}$ is a gamma distribution with known parameters, $\nu/2$ and 1/2; on the other hand, we can show that the sum of squares of OU processes can be shown to be a CIR process. The general form of a CIR SDE is shown in Equation (4):

$$dY_t = -b(Y_t - a)dt + \delta\sqrt{Y_t}\, dW_t \tag{4}$$

Where b, a, and δ have similar definitions to α, β, and σ in an OU process. The parameter b (strictly positive) corresponds to the speed of reversion to the long-run average a, and δ is the volatility. A major difference between the OU and CIR processes is the inclusion of $\sqrt{Y_t}$, which precludes the possibility of negative values for Y_t as long as a and b are positive. Also, the value of zero is excluded when the condition $\frac{2ab}{\delta^2} \geq 1$ is satisfied. The drift factor $-b(x_t - a)dt$ is similar to that of the OU process, which ensures the mean reversion of the variable Y_t towards the long-run value, a.

When $\alpha = 0$, Equation (4) reduces to $dX_{i,t} = -\beta X_{i,t}dt + \sigma dW_{i,t}$ i=1,2, …, ν. We can show the dynamic of $v_t = \sum_{i=1}^{\nu} X^2_{i,t}$ using Ito lemma and isometry $\sum_{j=1}^{\nu} X^2_{j,t} dW_{j,t} = \sqrt{\sum_{j=1}^{\nu} X^2_{j,t} dW_t}$ is expressed by a CIR process shown in Equation (5)

$$dv_t = (v\sigma^2 - 2\,\beta v_t)dt + 2\sigma\sqrt{v_t}\, dW_t \tag{5}$$

This shows that the summation of the zero-mean OU-squared process is also a CIR By comparing Equations (4) and (5), whence $ab = v\sigma^2$ and $b = 2\beta$ given the CIR parameters from OU process parameters: $a = \frac{v\sigma^2}{2\beta}$ and $\delta = 2\sigma$. This means that the speed of mean-reversion in the resulting CIR process is v times that of the OU process, where v is the number of OU processes that are being added. To drive Equation (5), we assumed that all the OU processes have identical parameters. In cases where OUs have different parameters, the resulting SDE can be shown to still be a CIR process (Chen and Scott (1992, 1995), Longstaff and Schwartz (1992) and (Brigo and Mercurio, 2001)).

The conditional expected value and variance of the CIR process given an initial point y_0 are shown in Equations (6) and (7) respectively (Cox et al., 1985).

$$E[Y_t|Y_0 = y_0] = a + (y_0 - a)e^{-bt} \tag{6}$$

$$Var[X_t|Y_0 = y_0] = y_0\frac{\delta^2}{b}\left(e^{-bt} - e^{-2bt}\right) + \frac{a\delta^2}{2b}(1 - e^{-bt})^2 \tag{7}$$

Asymptomatically, Equations (6) and (7) are $E[X_{t\to\infty}|Y_0 = y_0] = a$ and $Var[X_{t\to\infty}|Y_0 = y_0] = \frac{a\delta^2}{2b}$ respectively. Also, the distribution of a CIR, asymptomatically, is a gamma distribution with density function $f(Y_{t\to\infty}; a, b, \delta) = \frac{\rho^\tau}{\Gamma(\tau)} x_t^{\tau-1} e^{-\rho x_t}$. Thus, we can express the distribution of $Y_{t\to\infty}$ using the parameters of the CIR process by $Y_{t\to\infty} \sim Gamma\left(\frac{2ab}{\delta^2}, \frac{2b}{\delta^2}\right)$. Previously, we showed that the CIR generated

by S3OUP has an underlying gamma distribution $Gamma\ (\frac{v}{2}, \frac{1}{2})$. By placing these terms equal, we have $\frac{2ab}{\delta^2} = \frac{v}{2}$ and $\frac{2b}{\delta^2} = \frac{1}{2}$. As a result, $b = \frac{\delta^2}{4}$ and by substituting b in $\frac{2ab}{\delta^2}$, we have $a = v$, which is the long-run mean for the CIR process. This is an important conclusion, as it gives us the parameters of the underlying CIR process for test and evaluation of the process quality. In the next section, we will use this conclusion to discuss methods that quantify the performance of a CIR process.

4.0 DEVELOPING QUALITY METRICS

In section 4.1 we use the discussion of Section 3, to develop a method for evaluating the quality of the CIR process when its dynamic is explained by S3OUP. In section 4.2, we introduce phase I analysis and control charting of diffusion processes when the generalized method of moments (GMM) is used for parameter estimation.

4.1 Quantification of a CIR process performance generated by S3OUP

If we take samples of size *n* from independent realizations (or profile) of the CIR process, then according to the central limit theorem, we can conclude that the average of the CIR processes, denoted by $\overline{Y}_t$, asymptotically follows a normal distribution with the parameters given in Equation (8)

$$\bar{Y}_{t\to\infty} \sim N\left(v, \frac{2v}{n}\right) \tag{8}$$

Since the distribution of $\overline{Y}_{t\to\infty}$ is known, the natural tolerances of the underlying process can be readily established. The natural tolerance limits are those that contain 100(1-α)% of the quality characteristic. For $\overline{Y}_{t\to\infty}$, these limits are $v \pm Z_{\frac{\alpha}{2}}\sqrt{\frac{2v}{n}}$. Often a constant K is used instead of $Z_{\frac{\alpha}{2}}$ so that in a large number of samples, a fraction γ of the intervals $\bar{x} \pm Ks$ will include at least 100(1- α)% of the distribution (Montgomery, 2012). this statement can be summarized by Equation (9)

$$P(P(L \leq \bar{Y} \leq U) \geq 1 - \alpha) = \gamma \tag{9}$$

For example, if the number of OU processes that are building the CIR process is 2 ($v = 2$), $\alpha = 0.05$, *n=25*, $\gamma = 0.99$, then K = *2.972*, and the natural limit of this process is the interval $[0.811, 3.189]$. Thus, we can conclude that the interval encompasses 99% of the 95% confidence intervals that include the average of $\bar{Y}_{t\to\infty}$ processes. We can establish the natural tolerances of the underlying process as the lower and upper specification limits (LSL and USL). Using these limits, a measure of process quality would be the probability that the asymptotic average of a given process falls within the natural limits of the underlying process. Additionally, control charts can be established for monitoring the average and standard deviation of the $\bar{Y}_{t\to\infty}$ or $Y_{t\to\infty}$.

4.2 Capability Metrics

In the context of SPM, process capability metrics are defined as measures that determine what a process can produce. Given LSL and USL defined in Section 4.1, the measure of process capabilities, C_p, are defined in Equation (10)

$$C_p = \frac{USL - LSL}{6б} \tag{10}$$

Where б is the process standard deviation, and when it is unknown we use the estimated standard deviation $\hat{б}$ and can define $\hat{C}_p$ in Equation (11).

$$\hat{C}_p = \frac{USL - LSL}{6\hat{\sigma}} = \frac{USL - LSL}{6\sqrt{\frac{2v}{n}}} \quad (11)$$

Since $\hat{C}_p$, does not show deviations from the center of the process, a revised version is introduced called $\hat{C}_{pk}$, which is shown in Equation (12)

$$\hat{C}_{pk} = \frac{min(USL - \hat{\mu}, \hat{\mu} - LSL)}{3\hat{\sigma}} \quad (12)$$

Although $\hat{C}_{pk}$ captures deviation from the process mean, the value of standard deviation can dampen the effect of deviation from the mean. To avoid this problem a modified coefficient $C_{pm}$is given by Equation (13)

$$C_{pm} = \frac{USL - LSL}{6\tau} = \frac{USL - LSL}{6\sqrt{\sigma^2 + (\mu - \vartheta)^2}} = \frac{C_p}{\sqrt{1 + \xi^2}} \qquad \xi = \frac{\mu - \vartheta}{\sigma} \quad (13)$$

Where ϑ is the average of the target process. When mean and standard deviation are unknown, they are estimated from the process. By replacing Equation (11) in Equation (13), we can conclude Equation (14) for calculating the capability of $\overline{Y}_{t\to\infty}$.

$$\hat{C}_{pm} = \frac{\hat{C}_p}{\sqrt{1 + V^2}} \qquad V^2 = \frac{2\hat{b}(\hat{a} - v)^2}{\hat{a}\hat{\delta}^2} \quad (14)$$

When deviation from mean is zero, $\hat{C}_{pm}$=$\hat{C}_{pk}$. However, as the deviation from the target mean increases, $\hat{C}_{pm}$ decreases, making the process capability metric to decrease accordingly. Monitoring $\hat{C}_p$ and $\hat{C}_{pm}$ together can provide insights into the amount of shift in the asymptotic average of the process.

4.3 Control charts for Diffusion processes

In section 4.1, we introduced measuring and monitoring the quality characteristics of a CIR process resulted from S3OUP. In this section, we relax this assumption so that the control charting method introduced here can be used for any diffusion process.

Ideally, control charts for the estimates of the separate process parameters $\hat{a}$, $\hat{b}$, and $\hat{\delta}^2$ would provide a way to monitor them over time. However, when the parameter estimates are correlated, a joint chart is required for profile monitoring of the parameters. The joint distribution of the parameters depends on their estimator. In this paper, we use the Generalized Method of Moments (GMM) for parameter estimation of diffusion processes (Hansen, 1982) . Unlike Maximum Likelihood Estimation (MLE), GMM does not require complete knowledge of the distribution of the data. Instead, it matches the moments of an underlying model to an observed data value. Also, GMM is computationally less cumbersome than MLE (Chen et al. 1992). GMM estimates are consistent (i.e., as time approaches infinity, the estimated parameters converge to their true values) and are asymptotically Normal.

When different realization (profiles) of a diffusion process are independent of each other, control charting for a joint normal distribution is be appropriate. Harold Hoteling (1947) introduced T^2 distance as a measure that accounts for the covariance structure of a multivariate normal distribution, also known as Hoteling T^2. To reduce the problem of change detection from data to the change in model parameter estimates, the fitted model must adequately describe data. Therefore, to extend the application of T^2 control chart to monitor the parameter of diffusion processes, we introduce the application of the J-statistics chart in addition to the T^2 control charts. J-statistics is used to monitor the stability of the GMM estimator. When in the GMM method, parameters are over-identified (the number of moment conditions is more than the parameters) GMM estimation provides a method to test the specification of the proposed model. Details on the calculation of J-statistics are given in Hansen (1982). In section 5, we show the application of T^2 and J-statistics charts in developing the phase I control charts for a CIR process.

5.0 AN ILLUSTRATIVE EXAMPLE: APPLICATION IN AIRCRAFT TARGET LOCATION ERROR TEST AND EVALUATION

In this Section, we provide a real-life example that shows the application of the methods discussed in

Section 4 for an aircraft tracking performance test and evaluation. Target Location Error (TLE) is defined as the difference between the actual and the aircraft-system predicted location of the target. Target tracking systems are a major component of aircraft avionics systems. Currently, most systems that provide the target location estimation, are based on an underlying Kalman Filter. The errors from TLEs generated by a Kalman filter can be modeled by OU processes- due to the nature of Kalman Filter estimates' autocorrelation and tendency to revert to the long-run mean of zero. In this example, we assume a two-dimensional error in the horizontal plane— along-track and cross-track or latitude, longitude errors— that are independent. We first model the errors in two orthogonal directions using OU processes. Simulated horizontal errors associated with along-track and cross-track are denoted by OU_x and OU_y with parameters defined below:

$$OU_x \ : \ \beta_x = 0.2611, \alpha_x = 0 \ , \sigma_x = 1 \text{ and } X_0 = 15$$
$$OU_y : \ \beta_y = 0.2611, \alpha_y = 0 \ , \sigma_y = 1 \text{ and } X_0 = 1$$

We are interested in the quantification of the instrument performance in measuring the target location accurately. Figure 1 shows 30 realizations of the error along the x and y-axis in a period of 10 seconds where time steps are equal to 0.1 seconds.

As seen in table 1, GMM provides a close estimation of the expected long-run mean of 2 and Y_t has a δ^2 which is approximately four times its reverting speed. We previously showed that the natural tolerance of the CIR process was made from S3OUP when *v=2* is $[0.811 \quad 3.189]$. As a result, we can calculate the first quality metric, and that is, the probability of the given process asymptotically falls outside the natural tolerances of the underlying processes. To this end, we use the approximated parameters provided in Table 1 to calculate the distribution of $\mathrm{Y}_{t\to\infty}$, $\mathrm{Y}_{t\to\infty} \sim \mathrm{Gamma}\ (0.919, 0.49)$. Given the parameters of the gamma distribution, we can calculate the asymptotic expected value and variance of the $\mathrm{Y}_{t\to\infty}$ process $\mathrm{E}[\mathrm{Y}_{t\to\infty}|\mathrm{Y}_0 = \mathrm{y}_0] = 1.876$ and $\mathrm{Var}[\mathrm{Y}_t|\mathrm{Y}_0 = \mathrm{y}_0] = 1.957^2$. If we take samples of size 25, then $\overline{\mathrm{Y}}_{t\to\infty} \sim \mathrm{N}\left(1.878, \left(\frac{1.957}{5}\right)^2\right)$. Consequently, the probability that the sum of squares of errors is within the natural tolerances of the target process is $\mathrm{P}(\mathrm{LSL} \leq \overline{\mathrm{Y}}_{t\to\infty} \leq \mathrm{USL}) = \mathrm{P}(0.811 \leq \overline{\mathrm{Y}}_{t\to\infty} \leq 3.189) = 0.996$. Thus, when the threshold for accepting errors is 0.01, the process meets the specification.

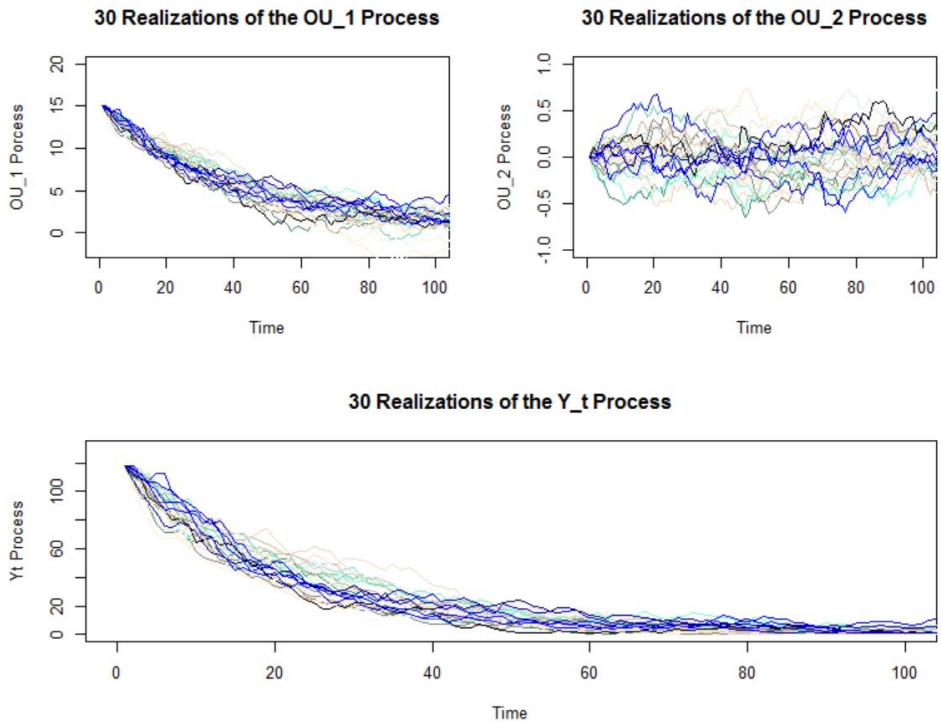

Figure 1 30 realization of the OU_x (top left) and OU_y (top right) and $Y_t = Z_x^2 + Z_y^2$ (bottom)

Table 1 estimation of parameters of $Y_t = Z_x^2 + Z_y^2$ process

	a	b	δ^2
GMM	1.875	0.05	0.204
GMM estimation lower confidence level ($\alpha = 0.05$)	1.746	0.045	0.199
GMM estimation Upper confidence level ($\alpha = 0.05$)	2.004	0.055	0.209

To measure the process capability, we use the metrics shown in equations (18), and (20) respectively:

$$\hat{C}_p = \frac{3.681 - 0.319}{6(0.391)} = 1.433$$

$$\hat{C}_{pm} = \frac{\hat{C}_p}{\sqrt{1 + \frac{(1.876 - 2)^2}{0.391^2}}} = 1.337$$

Figure 2 shows the underlying process density along with the distribution of the process in hand. As shown in the figure, the tighter blue curve implies that the standard deviation of the process is less than the underlying process. However, the process is slightly shifted to the left (average of 1.876 as opposed to 2). As a result, $\hat{C}_{pm}$ is smaller than $\hat{C}_p$, as it accounts for the shift of the process average. The vertical lines show the natural tolerances of the underlying process (red curve), which are assumed to be the upper and lower specifications limit for the process.

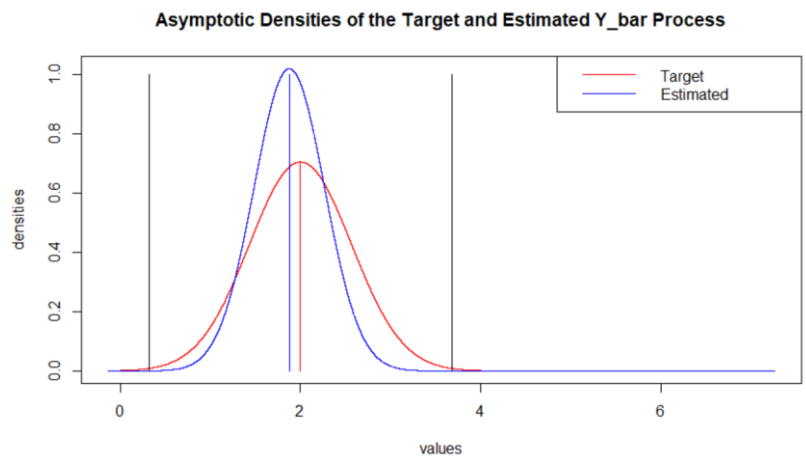

Figure 2 asymptotic densities of the underlying and $\bar{Y}_{t\to\infty}$ processes

In this example, we know the long-run mean of the S3OUP process is $\mathrm{v} = 2$. To develop control charts for monitoring of the CIR process, first, unstable estimates of the process parameters must be removed. To this end, we set-up the J-statistic chart to identify the GMM method instability. As shown in Figure 3 there are 4 estimates in which the moment condition does not hold, which are associated with profiles 4,10,16, and 30. Therefore, those estimates were removed from phase I analysis for setting up control limits.

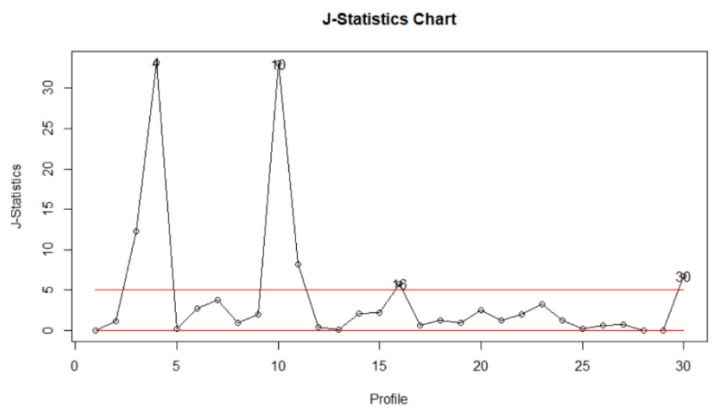

Figure 3 J-Statistic for the 30 estimates of $Y_t = Z_x^2 + Z_y^2$ process with GMM

Figure 4 shows the T^2 control charts, with (left chart) and without (right chart) the four unstable estimates. As shown in this figure, by removing the unstable estimates from the dataset, all estimates fall within the control limits of the multivariable control chart. Thus, these limits could be used for the phase II analysis of the diffusion process.

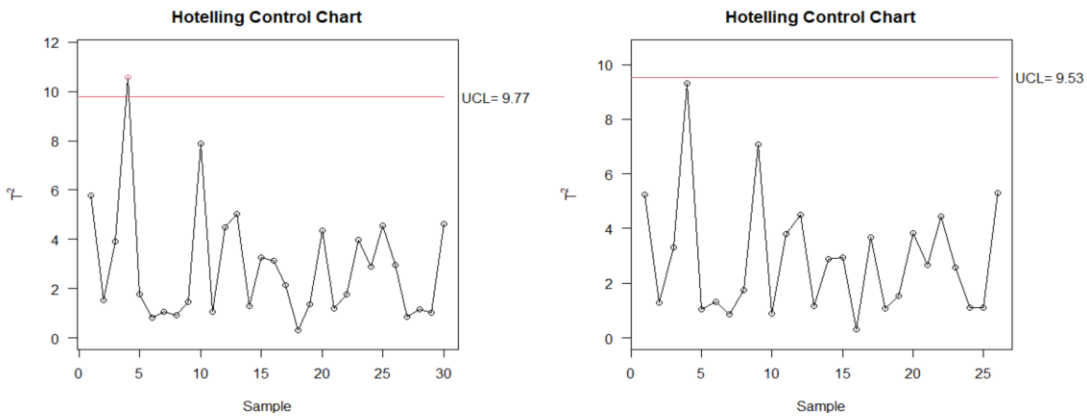

Figure 4 control charts for the joint distribution of the parameters before (left) and after (right) removing the unstable parameter estimates

Figure 5 shows control charts for the process based on the method described by Tsai (2014). As shown in this figure, limits for the average chart are too wide and in the variance chart, most of the points fall outside the limits. That is an indication that the T^2 chart, as well as the J-statistic in combination with Hotelling control charts are more appropriate methods for monitoring profiles of diffusion processes.

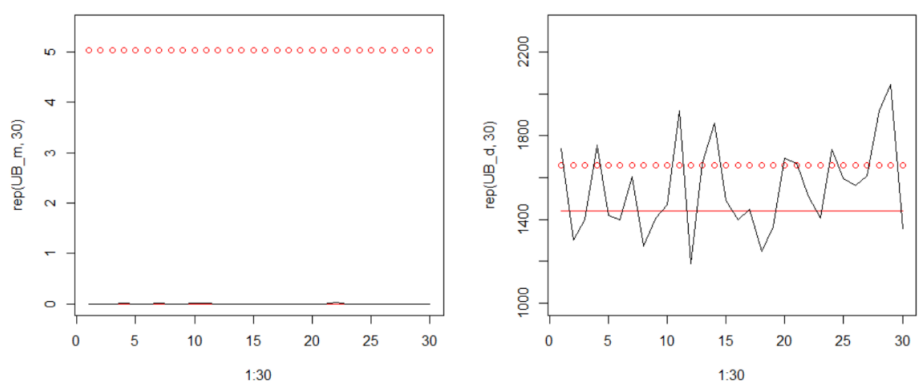

Figure 5 average (left) and variance (right) charts calculated by Tsai et al. (2014) method

6.0 CONCLUSION

In this work, we first quantified the performance of a CIR process when its dynamic is given by the sum of squares of standardized OU processes. Following this, we showed that the long-run mean of a S3OUP is given by the parameters of the OU processes, and can be used to develop quality metrics. When the assumption that the diffusion process is a S3OUP is relaxed, control charts for any diffusion process can be derived. To this end, we used a GMM estimator to estimate the parameters of the process and suggested monitoring of the process parameters as a joint multivariate normal distribution in combination with the J-statistics chart. The application of J-statistics is to evaluate and remove weak estimators of the process parameters. Future works include the extension of the result from Section 4.1 to cases where the dynamic of the CIR processes is not explained by S3OUP.

7.0 AUTHOR BIOS

Dr. Shokoufeh Mirzaei, is an associate professor of Industrial and Manufacturing Engineering at California

State Polytechnic University, Pomona. Dr. Mirzaei received her Ph.D. in Industrial Engineering with a minor in statistics from Wichita State University. After receiving her Ph.D., Dr. Mirzaei joined CGN global management consulting as a senior analytics consultant. In August 2012, she joined Cal Poly Pomona and since then she has published several peer-reviewed journals and conference papers in the area of applied optimization and analytics as well as machine learning. She has also worked with Lawrence Berkeley National Laboratory (summers of 2014, 2015, and 2016) and US Air Force Edwards Test Center (summer 2020) as a visiting faculty.

Erich Brownlow is a Mathematical Statistician working for the Department of the Air Force as part of the 812 Test Support Squadron at Edwards Air Force Base. Prior to joining the 812 TSS in 2017, Erich worked as an Electronic Warfare test and evaluation engineer also at Edwards AFB. He holds a B.S. degree in Discrete Mathematics from the Georgia Institute of Technology and a M.S. in Applied Statistics from California State University, Long Beach.

Dr. James Brownlow is a Mathematical Statistician for the U.S. Air Force. He has an A.B. in mathematics from Occidental College, an M.A. in mathematics from Kansas University, and a Ph.D. in applied statistics from U.C. Riverside. Dr. Brownlow currently provides test and evaluation support for Air Force programs at Edwards AFB, CA. His application interests include Bayesian models and machine learning.

Dr. Robert Poulson is the Chief Statistician to the 412 Test Wing of the U.S. Air Force. Prior to joining the Air Force in 2011, Dr. Poulson received his Ph.D. in Statistics at Kansas State University and his Masters in Statistics at Utah State University.

8.0 ACKNOWLEDGMENT

This work was supported by the Air Force Office of Scientific Research (AFOSR) under the Summer Faculty Fellowship Program, 2020.

9.0 REFERENCES

Abbas, T., Qian, Z., Ahmad, S., and Riaz, M. (2016). On monitoring of linear profiles using Bayesian methods. *Computers and Industrial Engineering*, Vol. 94, pp.245–268. https://doi.org/10.1016/j.cie.2016.02.007

Brigo, D., and Mercurio, F. (2001). Two-Factor Short-Rate Models. In D. Brigo and F. Mercurio (Eds.), *Interest Rate Models Theory and Practice* (pp. 127–171). Springer. https://doi.org/10.1007/978-3-662-04553-4_4

Chang, S. I., and Yadama, S. (2010). Statistical process control for monitoring non-linear profiles using wavelet filtering and B-Spline approximation. *International Journal of Production Research*, Vol. 48, No. 4, pp.1049–1068. https://doi.org/10.1080/00207540802454799

Chang, ShingI., Tsai, T.-R., Lin, DennisK. J., Chou, S.-H., and Lin, Y.-S. (2012). Statistical Process Control for Monitoring Nonlinear Profiles: A Six Sigma Project on Curing Process. *Quality Engineering*, Vol. 24, No. 2, pp.251–263. https://doi.org/10.1080/08982112.2012.641149

Chen, R.-R., and Scott, L. (1992). Pricing Interest Rate Options in a Two-Factor Cox–Ingersoll–Ross model of the Term Structure. *The Review of Financial Studies*, Vol. 5, No. 4, pp.613–636. https://doi.org/10.1093/rfs/5.4.613

Chen, R.-R., and Scott, L. (1995). Interest Rate Options in Multifactor Cox-Ingersoll-Ross Models of the Term Structure. *The Journal of Derivatives*, Vol. 3, No. 2, pp. 53–72. https://doi.org/10.3905/jod.1995.407938

Cox, J. C., Ingersoll, J. E., and Ross, S. A. (1985). A Theory of the Term Structure of Interest Rates. *Econometrica*, Vol. 53, No. 2, p.385. https://doi.org/10.2307/1911242

Feller, W. (1951). Two Singular Diffusion Problems. *Annals of Mathematics*, Vol.54, No.1, 173–182. JSTOR. https://doi.org/10.2307/1969318

Hansen, L. P. (1982). Large Sample Properties of Generalized Method of Moments Estimators. *Econometrica*, Vol. 50, No. 4, pp.1029–1054. JSTOR. https://doi.org/10.2307/1912775

Hansen, L. P., Heaton, J., and Yaron, A. (1996). Finite-Sample Properties of Some Alternative GMM Estimators. *Journal of Business and Economic Statistics*, Vol. 14, No. 3, pp.262–280. JSTOR. https://doi.org/10.2307/1392442

Jensen, W. A., and Birch, J. B. (2009). Profile monitoring via nonlinear mixed models. *Journal of Quality Technology*, Vol. 41, No. 1, pp.18–34.

Jensen, W. A., Birch, J. B., and Woodall, W. H. (2006). *Profile monitoring via linear mixed models*. Virginia Tech.

Jensen, W. A., Birch, J. B., and Woodall, W. H. (2008). Monitoring correlation within linear profiles using mixed models. *Journal of Quality Technology*, Vol. 40, No. 2, pp.167–183.

Jones, M. C., and Rice, J. A. (1992). Displaying the important features of large collections of similar curves. *The American Statistician*, Vol. 46, No. 2, pp.140–145.

Kang, L., and Albin, S. L. (2000). On-Line Monitoring When the Process Yields a Linear Profile. *Journal of Quality Technology*, Vol. 32, No. 4, pp.418–426. https://doi.org/10.1080/00224065.2000.11980027

Kim, K., Mahmoud, M. A., and Woodall, W. H. (2003). On the monitoring of linear profiles. *Journal of Quality Technology*, Vol. 35, No. 3, pp.317–328.

Longstaff, F., and Schwartz, E. S. (1992). Interest Rate Volatility and the Term Structure: A Two-Factor General Equilibrium Model. *Journal of Finance*, Vol. 47, No. 4, pp.1259–1282.

Mahmoud, M. A., and Woodall, W. H. (2004). Phase I Analysis of Linear Profiles with Calibration Applications. *Technometrics*, Vol. 46, No. 4, pp.380–391. JSTOR.

Moguerza, J. M., Muñoz, A., and Psarakis, S. (2007). Monitoring nonlinear profiles using support vector machines. *Iberoamerican Congress on Pattern Recognition*, pp.574–583.

Montgomery, D. C. (2012). *Statistical Quality Control* (7 edition). Wiley.

Noorossana, R., Amiri, A., and Soleimani, P. (2008). On the monitoring of autocorrelated linear profiles. *Communications in Statistics—Theory and Methods*, Vol. 37, No. 3, pp.425–442.

Noorossana, Rassoul, Saghaei, A., and Amiri, A. (2011). *Statistical Analysis of Profile Monitoring*. John Wiley and Sons, Incorporated. http://ebookcentral.proquest.com/lib/csupomona/detail.action?docID=693512

Ren, Z., An, B., and Yin, S. (2018). Process monitoring of nonlinear industrial process on quality variables based on kernel MPLS. *2018 3rd International Conference on Control and Robotics Engineering (ICCRE)*. https://doi.org/10.1109/iccre.2018.8376480

Shao, A. (n.d.). *A FAST AND EXACT SIMULATION FOR CIR PROCESS*. p.78.

Shewart, W. A. (1931). Economic Control of Quality of Manufactured Product ASQC (Milwaukee). *Revised*, 1980.

Tsai, T.-R., Chang, S. I., Chou, S.-H., Chiang, J.-Y., and Sung, W.-Y. (2014). *STATISTICAL PROCESS CONTROL FOR MONITORING A DIFFUSION PROCESS*. Vol. 6.

Vaghefi, A., Tajbakhsh, S. D., and Noorossana, R. (2009). Phase II monitoring of nonlinear profiles. *Communications in Statistics—Theory and Methods*, Vol. 38, No. 11, pp. 1834–1851.

Walker, E., and Wright, S. P. (2002). Comparing curves using additive models. *Journal of Quality Technology*, Vol. 34, No. 1, pp.118–129.

Wang, K., and Tsung, F. (2005). Using profile monitoring techniques for a data-rich environment with huge sample size. *Quality and Reliability Engineering International*, Vol. 21, No.7, pp. 677–688.

Williams, J. D., Birch, J. B., Woodall, W. H., and Ferry, N. M. (2007). Statistical Monitoring of Heteroscedastic Dose-Response Profiles from High-Throughput Screening. *Journal of Agricultural, Biological, and Environmental Statistics*, Vol. 12, Nov. 2, pp. 216–235. JSTOR.

Williams, James D., Woodall, W. H., and Birch, J. B. (2003). Phase I monitoring of nonlinear profiles. *Quality and Productivity Research Conference, Yorktown Heights, New York*.